# Magnetic phase transitions in nanostructures induced by shear stress under high pressure

*I. P. Suzdalev,[a]★ V. N. Buravtsev,[a] Yu. V. Maksimov,[a] A. A. Zharov,[b] V. K. Imshennik,[a] S. V. Novichikhin,[a] and V. V. Matveev[a]*

[a]*N. N. Semenov Institute of Chemical Physics, Russian Academy of Sciences, 4 ul. Kosygina, 119991 Moscow, Russian Federation. Fax: +7 (095) 137 8318. E-mail: suzdalev@chph.ras.ru*
[b]*N. D. Zelinsky Institute of Organic Chemistry, Russian Academy of Sciences, 47 Leninsky prosp., 119991 Moscow, Russian Federation. Fax: +7 (095) 135 5328. E-mail: zharov@ioc.ac.ru*

Magnetic phase transitions of the first and second order were revealed by Mössbauer spectroscopy in nanosystems of α- and γ-ferric oxides and metallic europium subjected to shear stress (240°) under high pressure (20 kbar). For α- and γ-ferric oxide nanoclusters, the Curie (Neel) points decreased to 300 K, whereas for nanostructured europium the Neel point increased from ~90 to 100 K. The thermodynamic model of magnetic phase transitions predicting a change in the character of magnetic phase transitions and a decrease (increase) in the critical Neel (Curie) points in nanoclusters was developed. The type of magnetic phase transitions and the change in the critical points were caused by defects in nanoclusters, whose maximum concentration was observed for the clusters with the 20—50 nm size range.

**Key words:** nanoclusters, nanosystems, ferric oxides, metallic europium, defects, magnetic phase transitions, shear stress under high pressure, Mössbauer spectroscopy, thermodynamic model.

The formation of nanoparticles is accompanied by considerable changes in the properties of solids. For example, the parameters of crystalline lattice, thermal capacity, melting point, as well as optical, electric, and other properties, change substantially in clusters ranging from 1 to 100 nm in size.[1—6] The magnetic characteristics of nanoclusters, such as the magnetization and shape of the hysteresis loop,[7] Curie and Neel points,[2] quantum magnetic tunneling that appears as the stepwise magnetization curves,[8] gigantic magnetic resistance,[9,10] *etc.*, differ considerably from the respective characteristics of bulky solids.

The properties of nanoclusters vary further when the isolated clusters are organized to form a nanostructure. The intercluster interaction and the influence of defects and strains at interfaces play the determining role in these processes. The cluster—matrix interaction can substantially change the properties of nanoclusters when the nanosystem is formed during polymerization or on the support surface.

The nanocluster system is characterized by the superparamagnetism phenomenon, which is caused by fluctuations of the magnetic moment of the whole cluster without a magnetic ordering loss. Thermal fluctuations and transition from the magnetic to superparamagnetic state can be observed by different methods. For example, magnetic methods monitor the superparamagnetic behavior and magnetic moment fluctuations during several seconds. Mössbauer spectroscopy allows the superparamagnetic properties to be studied within shorter time intervals ($10^{-8}$ s) and, correspondingly, nanoclusters with sizes of several nm can be studied.

Superparamagnetism is a reason for a decrease in the effective temperatures of magnetic phase transitions (MPT), *viz.*, Curie ($T_C$) and Neel ($T_N$) points, with decreasing cluster size. The blocking temperature (the temperature of the initial thermal fluctuations) also depends on the intercluster and cluster—matrix interactions. A superparamagnetic system is characterized by a smooth temperature plot of the magnetization (Langevin curve), which approaches zero at the $T_C$ or $T_N$ points. This plot is typical of the most part of bulky magnetics in which the MPT of the second order from the magnetic to nonmagnetic state occur in the temperature interval from 1 to 1000 K.[11] However, several substances, for example, some metal halides and oxides, rare-earth metals, and alloys (MnAs), exhibit MPT of the first order when the magnetic ordering and spontaneous magnetization disappear jumpwise at some critical temperature.[11] This phenomenon was explained in the framework of the thermo-

Published in Russian in *Izvestiya Akademii Nauk. Seriya Khimicheskaya,* No. 9, pp. 1848—1855, September, 2003.

1066-5285/03/5209-1950 $25.00 

dynamic theory of magnetization, which takes into account a distortion of the crystalline lattice with a pressure change and the appearance of strains on going through the Curie point.[12]

Unlike bulky samples, nanoclusters of ferric oxides and hydroxides also exhibited the MPT of the first order.[13—15] For example, the jump-like MPT in the 6—10 K temperature region were observed for the ferrihydrite nanoclusters in Polysorb pores.[15] These transitions were identified by Mössbauer spectra in which the nonbroadened hyperfine structure (HFS) lines from the magnetically ordered clusters coexisted with the nonbroadened lines of the quadrupole doublet from the clusters in the paramagnetic state. These spectra did not either contain the shift of lines of the magnetic HFS characteristic of superparamagnetism phenomena.

The character of MPT in nanocluster systems depends on the critical size of the cluster. For example, the cluster with sizes below critical becomes nonmagnetic, avoiding the superparamagnetic state.[13] We have previously[15] developed the thermodynamic theory of MPT of clusters, which takes into account the influence of surface tension and can explain the specific features of MPT in nanoclusters, including jump-like transitions in 1—2-nm clusters.[15]

Magnetic phase transitions of the first order were studied in the nanosystem of larger $\alpha$-$Fe_2O_3$ and $\gamma$-$Fe_2O_3$ clusters (20—50 nm, according to the atomic force microscopic data). This system was prepared by the solid state chemical reaction.[16] Despite considerable sizes, the MPT of the first order was observed at 120—300 K. As compared to that in the bulky material,[17] this transition was accompanied by a significant decrease in $T_C$ or $T_N$, and superparamagnetism was not observed in the Mössbauer spectra. In the framework of the thermodynamic model of the MPT, the decrease in the critical temperatures was attributed to the effect of pressure and strain (surface tension), which appear upon agglomeration of nanoclusters and formation of a nanosystem with a strong cluster—cluster interaction.[16]

Nanosystems can be prepared by a combination of individual (isolated) nanoclusters (molecular, gas clusters of fulleneres and others), formation of nanostructures from clusters formed in solid state chemical reactions, and inclusion of clusters into different matrices.[2,15] Nanostructures can also be formed when a bulky solid is shattered by different methods. These methods include the mechanochemical treatment using high-energy mills and shear stress under high pressure.[18]

In the present work, we used Mössbauer $^{57}$Fe and $^{151}$Eu spectroscopy in the 78—300 K temperature interval to study the MPT in nanosystem **1** consisting of clusters of $\alpha$- and $\gamma$-ferric oxides and acrylamide and nanosystem **2** containing metallic europium clusters with additives of clusters of $\alpha$- and $\gamma$-ferric oxides and adamantane molecules, which were treated with shear stress (240°) under high pressure (20 kbar). The obtained results were compared to the results of calculations by the thermodynamic model. The latter makes it possible to reveal the temperature dependence of the magnetization for nanosystems consisting of clusters of different sizes arranged at different distances from each other and with different concentrations of defects.

## Experimental

Two types of nanosystems were studied: those based on nanoclusters of $\alpha$- and $\gamma$-$Fe_2O_3$ 20—50 nm in size (**1**) and those based on metallic europium (**2**). Nanosystem **1** included 20—50-nm nanocluster samples of $\alpha$- and $\gamma$-$Fe_2O_3$ (**1.1**) and 20—50-nm $\alpha$- and $\gamma$-$Fe_2O_3$ nanoclusters with an additive of 50% monomeric acrylamide (**1.2**). Nanosystem **2** consisted of samples of metallic Eu (**2.1**), metallic Eu with an additive of 1% $\alpha$- and $\gamma$-$Fe_2O_3$ nanoclusters with size ranging from 20 to 50 nm (**2.2**), and metallic Eu with an additive of 10% adamantane (**2.3**). The $\alpha$- and $\gamma$-$Fe_2O_3$ nanoclusters (20—50 nm) were synthesized by thermal decomposition of ferric oxalate.[16] Powdered samples were compacted to pellets and treated with shear stress under high pressure to induce acrylamide polymerization in nanostructure **1.2**. The samples of nanosystem **2** were treated similarly.

A high-pressure installation with the Bridgeman anvils produced pressures up to 50 kbar with the simultaneous accumulation of the total shear with an increment change of 10° during 5 s.[18] A pressure of 20 kbar with the turn angle of the anvils (diameter 9 mm) from 120° to 240° and a sample thickness of 100 μm were used in experiments. The shear deformation $\tau$ was calculated from the equation $\tau = \theta r/h$, where $\theta$ is the turn angle of the anvils in rad, $r$ is the radius of the anvils in mm, and $h$ is the sample height in mm; the turn angle 240° corresponds to $\tau = 190$.

Mössbauer $^{57}$Fe and $^{151}$Eu spectra were obtained on a Wissel technique with the $^{57}$Co/Rh and $^{151}Sm_2O_3$ radiation sources with activities of ~10 and 100 mCi, respectively. The spectra were analyzed by components using standard least-squares programs. Isomeric shifts were counted from the center of the magnetic HFS lines for $\alpha$-Fe and from the center of the $Eu_2O_3$ monoline. Temperature measurements were carried out in an Oxford Instruments Mössbauer cryostat in a temperature region of 78—300 K.

## Results and Discussion

**Analysis of Mössbauer spectra.** The Mössbauer spectra of the samples of nanosystem **1** obtained at ~20 °C are presented in Fig. 1. The spectrum of sample **1.1** (see Fig. 1, *a*) consists of the magnetic HFS lines of $\alpha$- and $\gamma$-$Fe_2O_3$ and a nonmagnetic quadrupole doublet. The parameters of the spectra are presented in Table 1.

Shear stress under high pressure on nanosystem **1.1** insufficiently changes the spectrum and gives rise only to a decrease in the relative content of the paramagnetic doublet to $A = 0.28$ (see Fig. 1, *b*). The change in the ratio

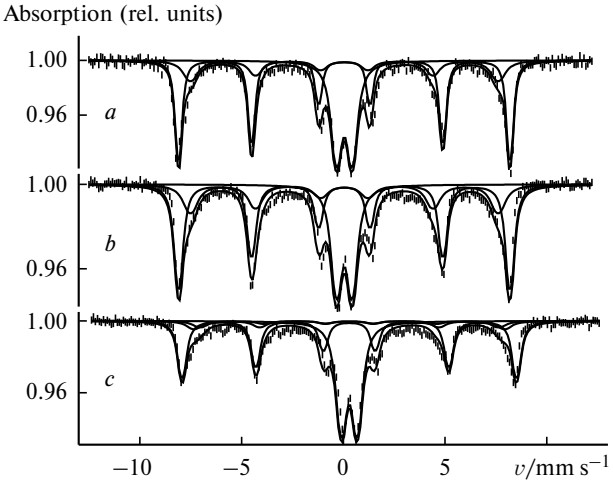


**Fig. 1.** Mössbauer $^{57}$Fe spectra of samples of nanosystem **1** at ~20 °C: sample **1.1** (*a*); sample **1.1** upon a pressure of 20 kbar with the turn angle of anvils 240° (*b*); sample **1.2** upon a pressure of 20 kbar with the turn angle of anvils 240° (*c*); here and in Figs. 2—4 $\upsilon$ is the velocity of the radiation source relatively to the absorber.

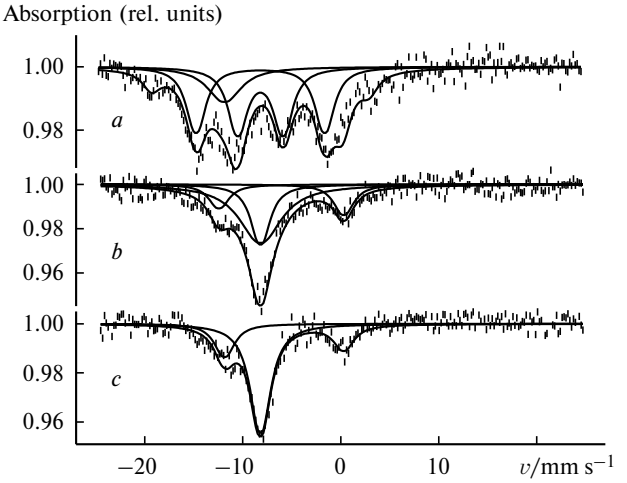


**Fig. 2.** Mössbauer $^{151}$Eu spectra of nanostructure **2.1** at $T = 77$ (*a*), 90 (*b*), and 100 K (*c*) upon a pressure of 20 kbar with the turn angle of anvils 120°.

of the magnetic HFS fraction to the paramagnetic doublet in nanosystem **1.2** is much more noticeable (see Fig. 1, *c*). In fact, in the loaded sample the fraction of the paramagnetic doublet increased to $A = 0.42$. It is known that the shear stress under high pressure (~20 kbar) results in acrylamide polymerization.[19] After the pressure is eliminated, the shear deformations in the polymer remain unchanged on the sample of the α- and γ-$Fe_2O_3$ nanoclusters, preventing their recrystallization and recovery of the initial phase equilibrium. As a result, the shear stress in the α- and γ-$Fe_2O_3$ nanoclusters in the presence of acrylamide increases from $0.8 \cdot 10^3$ to $1.4 \cdot 10^3$ kg cm$^{-2}$, which causes a substantial change in the spectrum.

The Mössbauer $^{151}$Eu spectra of nanostructure **2.1** at $T = 77$, 90, and 100 K after shear stress under high pressure are presented in Fig. 2. The parameters of the spectra are presented in Table 2.

The spectrum at $T = 77$ K consists of the magnetic HFS lines from metallic Eu in the magnetically ordered state, a broadened line from EuO, and a line from $Eu_2O_3$. The unresolved components of these lines appear due to the complicated nuclear transitions of $^{151}$Eu ($\pm 7/2 \rightarrow \pm 5/2$).[20] The Mössbauer spectrum at $T = 90$ K contains four components: a singlet from metallic Eu in the nonmagnetic (paramagnetic) state with a narrow line, a broadened line from metallic Eu, and two lines from EuO and $Eu_2O_3$. The Mössbauer $^{151}$Eu spectra at $T =$ 100 K consist of three components corresponding to the nonmagnetic state of metallic Eu with a narrow line and lines from EuO and $Eu_2O_3$. It is noteworthy[21,22] that for the unloaded sample of metallic Eu the critical temperature for the MPT of the first order is $T_N = 87$ K; the shape of the spectrum is similar to that presented in Fig. 2, *c*.

The Mössbauer $^{151}$Eu spectra of nanosystems **2.1**, **2.2**, and **2.3** at $T = 90$ K after shear stress under high pressure

**Table 1.** Parameters of the spectra of nanostructure **1.1** at $T = 300$ K

| Component of spectrum | δ±0.03 | $q$ ($\Delta E_Q$)±0.03 | $H_{in}$±0.5 | $A$±0.05 |
|---|---|---|---|---|
| | mm s$^{-1}$ | | /T | |
| Sextet of α-$Fe_2O_3$ | 0.24 | 0.20 | 51.5 | 0.50 |
| Sextet of γ-$Fe_2O_3$ | 0.39 | 0.02 | 48.8 | 0.17 |
| Doublet | 0.39 | (0.74) | — | 0.33 |

*Note.* δ is the isomeric shift, $q$ is the quadrupole shift, $\Delta E_Q$ is the quadrupole splitting, $H_{in}$ is the internal magnetic field on $^{57}$Fe, and $A$ is the relative surface area under the spectrum.

**Table 2.** Parameters of the spectra of nanostructure **2.1** at $T = 77$, 90, and 100 K

| $T$/K | Component of spectrum | δ±0.1 | Γ±0.1 | $A$±0.05 |
|---|---|---|---|---|
| | | mm s$^{-1}$ | | |
| 77 | Eu (magnet.)* | −8.2 | 2.2 | 0.68 |
| | EuO | −11.9 | 4.0 | 0.19 |
| | $Eu_2O_3$ | 0.2 | 2.3 | 0.13 |
| 90 | Eu (paramagn.) | −8.2 | 2.2 | 0.24 |
| | Eu (br) | −8.2 | 5.0 | 0.51 |
| | EuO | −11.9 | 2.3 | 0.12 |
| | $Eu_2O_3$ | 0.3 | 2.3 | 0.13 |
| 100 | Eu (paramagn.) | −8.2 | 2.4 | 0.69 |
| | EuO | −11.8 | 2.3 | 0.17 |
| | $Eu_2O_3$ | 0.2 | 2.3 | 0.13 |

*Note.* δ is the isomeric shift, Γ is the linewidth, and $A$ is the relative surface area under the spectrum.
* $H_{in}$ (internal magnetic field on $^{151}$Eu) = 16.0±1.5 T.

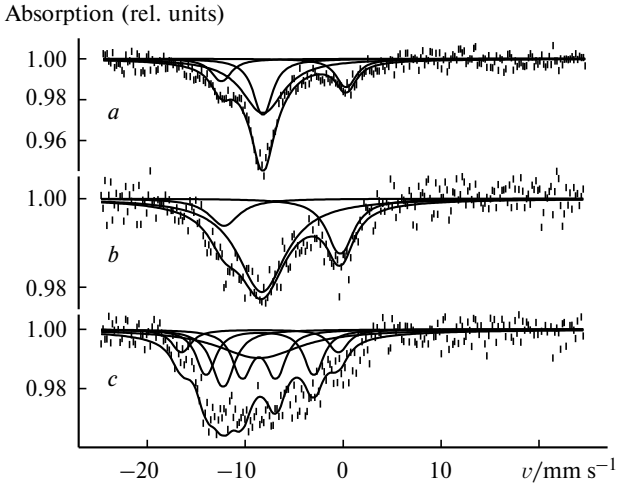


**Fig. 3.** Mössbauer $^{151}$Eu spectra of nanostructures **2.1** (*a*), **2.2** (*b*), and **2.3** (*c*) at $T = 90$ K upon a pressure of 20 kbar with the turn angle of anvils 120°.

are shown in Fig. 3. The parameters of the spectra are presented in Table 3.

The spectrum of sample **2.1** including four components has already been described (see Fig. 2, *b* and Table 2). The spectrum of nanosystem **2.2** consists of three components: a broad line of metallic Eu and lines from EuO and $Eu_2O_3$. The spectrum of nanosystem **2.3** contains three components corresponding to lines of the magnetic HFS of metallic Eu in the magnetically ordered state, a very broad monoline of metallic Eu, and a monoline of EuO.

The Mössbauer $^{57}$Fe spectrum of nanostructure **2.2** at $T = 300$ K after shear stress under high pressure (Fig. 4) demonstrates an almost complete magnetic ordering loss in the ferric oxide clusters. In fact, the spectrum exhibits only a quadrupole doublet with $\delta =$ $0.37\pm0.03$ mm s$^{-1}$ and $\Delta E_Q = 0.68\pm0.03$ mm s$^{-1}$, which characterizes the paramagnetic state of the $Fe^{3+}$ ion in the clusters.

**Table 3.** Parameters of the spectra of nanosystems **2.1**, **2.2**, and **2.3** at $T = 90$ K

| Nano-system | Component of spectrum | δ±0.1 | Γ±0.1 | *A*±0.05 |
|---|---|---|---|---|
| | | mm s$^{-1}$ | | |
| **2.1** | Eu (paramagn.) | −8.2 | 2.2 | 0.24 |
| | Eu (br) | −8.2 | 5.0 | 0.51 |
| | EuO | −11.9 | 2.3 | 0.12 |
| | $Eu_2O_3$ | 0.3 | 2.3 | 0.13 |
| **2.2** | Eu (br) | −8.3 | 6.0 | 0.67 |
| | EuO | −11.4 | 3.1 | 0.13 |
| | $Eu_2O_3$ | 0.0 | 3.7 | 0.20 |
| **2.3** | Eu (magnet.)* | −8.3 | 2.2 | 0.53 |
| | Eu (br) | −8.3 | 10.0 | 0.31 |
| | EuO | −12.1 | 2.3 | 0.16 |

*Note.* For designations, see Table 2.
* $H_{in} = 16.0\pm1.5$ T.

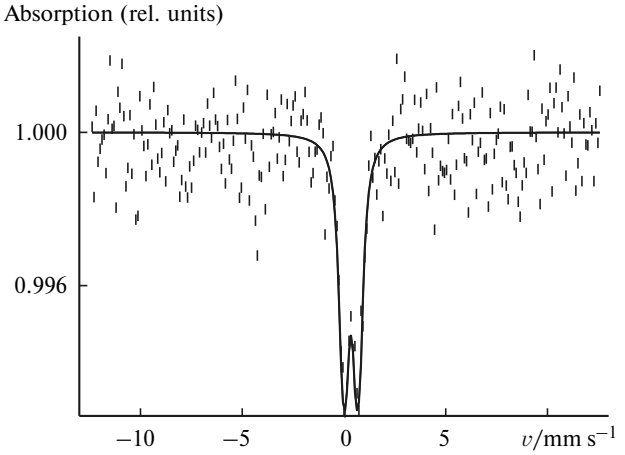


**Fig. 4.** Mössbauer $^{57}$Fe spectrum of nanostructure **2.2** at ~20 °C upon a pressure of 20 kbar with the turn angle of anvils 240°.

Analysis of the experimental data suggests the following. First, the MPT of the first order (jump-like magnetic transitions) are observed in nanocluster system **1.1** subjected to shear stress under high pressure. This is a consequence of the fact that in the nanosystem under study, as in analogous nanosystems,[16,17] an increase in the temperature of measurement from 77 to 300 K results in the transition of the ferric oxide clusters from the magnetically ordered to paramagnetic state without line broadening, *i.e.*, without any properties of the superparamagnetic behavior of the system. Second, the critical MPT temperatures for ferric oxides ($T_C$ or $T_N$) in nanocluster systems **1.1**, **1.2**, and **2.2** are much lower than the MPT temperatures of bulky samples of α- and γ-$Fe_2O_3$ ($T_C$, $T_N$ ~700—850 K). Additives of acrylamide (sample **1.2**) or metallic Eu (sample **2.2**) further decrease the critical MPT points for the $Fe_2O_3$ clusters. Third, the sample of loaded (nanostructured) metallic Eu (**2.1**) is characterized by the MPT of the second order. This is inferable from the fact that above the critical transition temperature (~90 K) the spectrum shows a superposition of the broadened line from nonmagnetic Eu and magnetic HFS lines from magnetically ordered Eu. Thus, the MPT temperature $T_C$ for a part of nanostructured Eu is higher (~100 K) than the MPT temperature of bulky Eu (87 K). Fourth, the addition of 1% α- and γ-$Fe_2O_3$ nanoclusters (sample **2.2**) or 10% adamantane (sample **2.3**) to metallic Eu further increases $T_C$, which is especially pronounced for nanosystem **2.3** (see Table 3).

**Thermodynamic model of magnetic phase transitions.** Thus, substances capable of MPT of the second order (α-, γ-$Fe_2O_3$) in the crystalline state and characterized by the Langevin-type temperature curves of magnetization undergo MPT of the first order with a simultaneous jump-

like decrease in $T_C$ and $T_N$, when in the nanostructured state.

Specific features of the nanosystems can be discussed in the framework of the thermodynamic MPT model, which takes into account the size of clusters composing the systems, intercluster interactions, and deficiency of the cluster structure.[23]

Unlike atoms and molecules that form the crystalline lattice of solids, nanoclusters forming a nanostructure possess their intrinsic surface. Therefore, when the influence of defects on the properties of a nanosystem is considered, the concept of their thermodynamic concentration should be complemented by the chemical potential and an excessive energy of the cluster surface. The latter results in the appearance of an excessive pressure, which is[24,25] ~$10^9$ Pa for a cluster 1 nm in size.

A cluster can be considered as a mixture of atoms of the main structure, defects of the structure, and atoms of an admixture and/or vacancies. When a nanosystem is formed, all "disturbers" of the main structure (defects) can be redistributed between the cluster volume and intercluster medium. The system is equilibrated when the chemical potentials (μ) of defects inside the cluster

$$\mu_v = \mu_v^0(p) + kT\ln c_v \qquad (1)$$

and in the intercluster medium

$$\mu_s = \mu_s^0(p_0) + kT\ln c_s. \qquad (2)$$

become equal. Here $\mu_v^0$ and $\mu_s^0$ are the standard chemical potentials, $p$ and $c_v$ are the pressure and concentration of defects inside the cluster, $p_0$ and $c_s$ are the pressure and concentration of defects in the intercluster medium, and $k$ is the Boltzmann constant.

Assuming that the complete total number of defects in the system $n_0$ is constant, the $c_s$ and $c_v$ concentrations are related as follows:

$$c_s = c_0 - (1/q)c_v. \qquad (3)$$

In this correlation, the maximum possible concentration of defects in the intercluster medium $c_0 = n_0/\{(4\pi/3)\cdot[(R+r)^3 - R^3]\}$ is considered constant and independent of the cluster size, and the function of the cluster radius $q$ is given by

$$q(R) = (1 + r/R)^3 - 1, \qquad (4)$$

where $r$ is the layer thickness of the intercluster medium, and $R$ is the cluster radius.

In the calculation of the equilibrium concentration of an admixture in the cluster, one should take into account that the excessive pressure in the cluster is

$$p - p_0 = 2\alpha/R, \qquad (5)$$

where α is the surface tension coefficient of the cluster boundary. Then from the condition $\mu_v = \mu_s$ and taking into account Eqs. (1)—(5) we find that at equilibrium

$$\frac{c_v}{c_0} = \left\{\frac{1}{(1 + r/R)^3 - 1} + \exp\left[\frac{\Delta\mu^0(p_0) + (2\alpha v/aR)}{kT}\right]\right\}^{-1}, \qquad (6)$$

where $v$ is the defect volume, and $a$ is the lattice increment.

**Table 4.** Parameters of calculation by Eq. (6) of the $c_v/c_0 = f(R/a)$ plot presented in Fig. 5

| Parameter | Cluster | |
|---|---|---|
| | metal | oxide |
| $a$/m | $2\cdot10^{-10}$ | $5\cdot10^{-10}$ |
| $\alpha$/N m$^{-1}$ | 1 | 1 |
| $T$/K | 100 | 300 |
| $\Delta\mu^0$ | 0 | 0 |

*Note.* $a$ is the lattice increment (equal to the atomic layer thickness), α is the surface tension, $T$ is the temperature of measurement, and $\Delta\mu^0$ is the difference of chemical potentials.

The $c_v/c_0 = f(R/a)$ plot calculated by formula (6) with the parameters presented in Table 4 is shown in Fig. 5.

The $c_v/c_0$ plot has a maximum because with decreasing cluster size, on the one hand, the fraction of the surface (defect) structure in the total volume of the system increases. On the other hand, defects are released from the cluster volume due to an increase in the surface pressure. The well known effect of removing and healing defects with a decrease in the cluster size predominates in the system. The process begins from some size corresponding to the maximum in the curve in Fig. 5.

The presence of a maximum in the plot of the defect concentration *vs.* cluster size specifically is reflected on the temperature plots of the magnetization of clusters with different sizes. Taking into account the magnetic

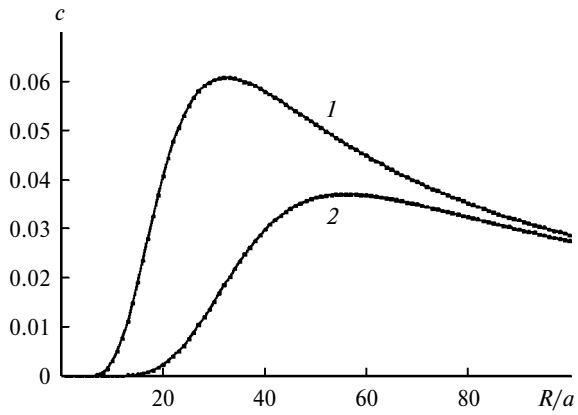


**Fig. 5.** Plot of the relative concentration of defects in the cluster ($c$) *vs.* relative cluster radius ($R/a$) for metals (*1*) and oxides (*2*) ($R$ is the cluster radius, $a$ is the lattice increment).

interaction of clusters, the thermodynamic potential of the magnetic clusters—medium—defects nanosystem is written as a sum of two terms

$$G = G_c + G_m, \quad (7)$$

where the term $G_c = \nu_V N_V + \nu_s N_s + \mu_v(p_0)n_v + \mu_s(p_0)\cdot(n_0 - n_v) + \alpha S(n)$ is the thermodynamic potential of the cluster—medium—defects system without magnetization, and the term $G_m = -HM - 0.5NkT_C m^2 + NkT\{0.5\ln[(1 - m^2)/4] + m\ln[(1 + m)/(1 - m)]\}$ takes into account magnetic interactions. Here $H$ is the external magnetic field, $M$ is the magnetic moment of the cluster, $m = M/M_0$ is the relative magnetic moment of the cluster, $N_V$ is the number of atoms of the main structure in the cluster, $N$ is the number of atoms of the main structure with a spin of 1/2 in the cluster, $N_s$ is the number of atoms in the intercluster medium for one cluster, $n_0$ is the total number of defects in the system (cluster + medium), $n_v$ is the number of defects in the cluster, $c_v = n_v/N_V$ is the concentration of an admixture in the cluster, $c_s = (n_0 - n_v)/N_s$ is the concentration of an admixture at the external boundary of the cluster, $v$ is the defect volume, $\nu_V$ is the chemical potential of the main structure, $\nu_s$ is the chemical potential of the main structure of the intercluster medium, $\mu_v$ and $\mu_s$ are the chemical potentials of defects in the cluster and outside the cluster (see Eqs. (1) and (2)), $\alpha$ is the surface tension of the cluster—medium boundary, and $S$ is the surface area of the cluster surface.

Under the condition that $dN_V = 0$, $dN_s = 0$, and $dn_v = 0$,

$$dG_c = \mu_v(p_0)dn_v - \mu_s(p_0)dn_v + \alpha dS(n_v)$$

or

$$dG_c = [\Delta\mu^0 + kT\ln(c_v/c_s)]dn_v + \alpha(dS/dn_v)dn_v, \quad (8)$$

where $\Delta\mu^0(p_0) = \mu_v{}^0(p_0) - \mu_s{}^0(p_0)$.

The derivative $dS/dn_v = v dS/dV$, because the cluster volume $V = Nw + n_v v$, where $dV = v dn_v$ ($w$ is the unit cell volume of the main structure).

For a spherical cluster $dS/dV = 2/R$, hence

$$dG_c = \{[\Delta\mu^0(p_0) + kT\ln(c_v/c_s)] + 2\alpha v/R\}dn_v. \quad (9)$$

Introducing the molar potential value

$$g_c = G_c/N_V, \quad (10)$$

we obtain $dg_c/dc_v = [\Delta\mu^0(p_0) + kT\ln(c_v/c_s)] + v\delta p$ and $dg_c/dm = 0$, where $\delta p = 2\alpha v/R$ is the excessive capillary pressure in the cluster. The molar value of the magnetic term takes the form

$$g_m = G_m/Ng_m = -HM/N_V - 0.5ukT_C m^2 + ukT\{0.5\ln[(1 - m^2)/4] + m\ln[(1 + m)/(1 - m)]\}, \quad (11)$$

where $u = N/N_V$ is the spin concentration in the cluster.

The first term of this equation, $-HM/N_V$, is the magnetic dipole energy of the cluster ($M$) in the overall magnetic field of its neighbors referred to one atom of the main structure. Summarizing the fields of six nearest neighbors, one can estimate the external field intensity on the cluster as

$$H \approx 2(2M/L^3) + 4(M/L^3) = 8(M/L^3), \quad (12)$$

where $L = 2R + r$ is the distance between the centers of the clusters. The magnetic moment of the cluster can be presented as $M = mM_0$, where $M_0 = p_s N$ is the maximum magnetic moment of the cluster, and $p_s$ is the magnetic moment of the atom. Therefore,

$$HM/N_V = 8[(p_s N)^2/(N_V L^3)]m^2 = 8(p_s{}^2 Nu/L^3)m^2$$

and

$$g_m = -8(p_s{}^2 Nu/L^3)m^2 - 0.5ukT_C m^2 + ukT\{0.5\ln[(1 - m^2)/4] + m\ln[(1 + m)/(1 - m)]\}. \quad (13)$$

Evidently, the critical temperature $T_C$ depends on the deficiency of the cluster structure, *i.e.*, on the $c_v$ value. In the linear approximation near $c_v = 0$ (this corresponds to the critical temperature for the defect-free cluster $T_c{}^0$), this dependence can be presented as follows:

$$T_C = T_c{}^0(1 + \beta c_v). \quad (14)$$

Therefore,

$$dg_m/dc_v = -0.5ukT_c{}^0\beta m^2, \quad (15)$$

$$dg_m/dm = -16(p_s{}^2 Nu/L^3)m - ukT_c{}^0(1 + \beta c_v)m + 0.5ukT\ln[(1 + m)/(1 - m)]. \quad (16)$$

Correspondingly,

$$g = g_c + g_m. \quad (17)$$

The temperature dependence of the relative magnetization $m$ can be determined from the conditions of a minimum of the thermodynamic potential with respect to $m$ and $c_v$ corresponding to the particular equilibria of the system with respect to $c_v$

$$dg/dc_v = [\Delta\mu^0(p_0) + kT\ln(c_v/c_s)] + v\delta p - 0.5ukT_c{}^0\beta m^2 = 0 \quad (18)$$

and with respect to $m$

$$dg/dm = -16(p_s{}^2 Nu/L^3)m - ukT_c{}^0(1 + \beta c_v)m + 0.5ukT\ln[(1 + m)/(1 - m)] = 0. \quad (19)$$

Introducing the designation $e(m) = (1/m)\ln[(1 + m)/(1 - m)]$, the conditions of particular equilibria with respect to $c_v$ and $m$ can be presented as follows:

$$c_v = c_s\exp[(-\Delta\mu^0/kT_c^0 - v\delta p/kT_c^0 + 0.5u\beta m^2)(T_c^0/T)],$$

$$0.5e(m)(T/T_c^0) = 1 + \beta c_v + 16p_s^2(N/L^3)/kT_c^0,$$

or, considering that

$$c_s = c_0 - (1/q)c_v,$$

$$c_v = c_0q(R)/\{1 + q(R)\exp[(\Delta\mu^0/kT_c^0 + v\delta p/kT_c^0 - 0.5u\beta m^2)(T_c^0/T)]\}0.5e(m)(T/T_c^0) = 1 + \beta c_v + 16p_s^2(N/L^3)/kT_c^0. \quad (20)$$

Introducing this expression for $c_v$, we obtain the condition of equilibrium of the system

$$(\beta c_0)q(R)/\{1 + q(R)\exp[(\Delta\mu^0/kT_c^0 + v\delta p(R)/kT_c^0 - 0.5(u\beta)m^2)(T_c^0/T)]\} + 1 - 0.5e(m)(T/T_c^0) + 16p_s^2(N/L^3)/kT_c^0 = 0. \quad (21)$$

The last term of the equation describing the dipole-dipole interaction in the system of clusters can be converted as follows:

$$16p_s^2(N/L^3)/kT_c^0 = 16(4\pi/3)p_s^2n_ku/(2 + r/R)^3/kT_c^0, \quad (22)$$

where $n_k = N_V/(4\pi R^3/3)$ is the density of the number of atoms of the main structure.

Finally, we obtain

$$(\beta c_0)q(R)/\{1 + q(R)\exp[(\Delta\mu^0/kT_c^0 + v\delta p(R)/kT_c^0 - 0.5(u\beta)m^2)(T_c^0/T)]\} + 1 - 0.5e(m)(T/T_c^0) + 16(4\pi/3)p_s^2n_ku/(2 + r/R)^3/kT_c^0 = 0. \quad (23)$$

Since

$$q(R) = [(1 + r/R)^3 - 1] = [(1 + (r/a)(a/R))^3 - 1]$$

and

$$v\delta p(R)/kT_c^0 = 2\alpha v/RkT_c^0 = (2\alpha v/akT_c^0)(a/R),$$

the system contains seven pairs of independent parameters: $\beta c_0$, $m = \Delta\mu^0/kT_c^0$, $u\beta$, $R/a$, $r/a$, $(2\alpha v/a)/kT_c^0$, and $p_s^2n_ku/kT_c^0$.

The resulting condition of equilibrium (23) relates implicitly the magnetization $m$ and temperature $T$. It is a transcendent equation with respect to both $T$ and $m$, *i.e.*, it cannot be allowed in quadratures, and hence, the solution can be obtained either numerically or approximately. The thermodynamic, structural, and magnetic parameters of the system are presented in Table 5.

**Table 5.** Thermodynamic, structural, and magnetic parameters of the system for calculation of the temperature plot of magnetization by Eq. (23)

| Parameter | Cluster | |
|---|---|---|
| | metal | oxide |
| $a$/m | $2\cdot10^{-10}$ | $5\cdot10^{-10}$ |
| $c_0$ | 0.33 | 0.33 |
| $u$ | 1 | 0.4 |
| $\alpha$/N m$^{-1}$ | 1 | 1 |
| $T_c^0$/K | 100 | 800 |
| $\beta$ | −30 | −30 |
| $\Delta\mu^0$ | 0 | −1.3 |
| $p_s$/J s A$^{-1}$ | $1\cdot10^{-26}$ | $2\cdot10^{-26}$ |
| $n_k$/m$^{-3}$ | $1\cdot10^{29}$ | $7\cdot10^{29}$ |

*Note.* $R/a$ = 500, 400, 300, 200, 100, 50, 25, 12, 6; $c_0$ is the maximum concentration of defects, $u$ is the spin concentration, $T_c^0$ is the temperature of transition in the defect-free cluster, $\beta$ is the coefficient equal to $dT_C/dc_v$, $p_s$ is the magnetic moment of atom, and $n_k$ is the density of atoms in the main structure.

The plots of the relative magnetization ($m$) *vs.* relative temperature $T/T_c^0$ for ferric oxide are presented in Fig. 6 as an example. It was assumed in calculations that $p_s$ has an order of the Bohr magneton ($\mu_B = 10^{-26}$ J s A$^{-1}$) and $n_k \approx 10^{-29}$ m$^{-3}$.

**Results of application of the thermodynamic model.** The results of calculations by the thermodynamic model explain all magnetic effects observed in the nanostructures under study. According to the model for the ferric oxide clusters of 20—50 nm, the MPT of the first order should be observed (z-like curves). The magnetization of these clusters disappears jumpwise at a temperature higher than $T_C$. The $T_C$ value also depends on the size of the clusters composing the system. When the cluster size is

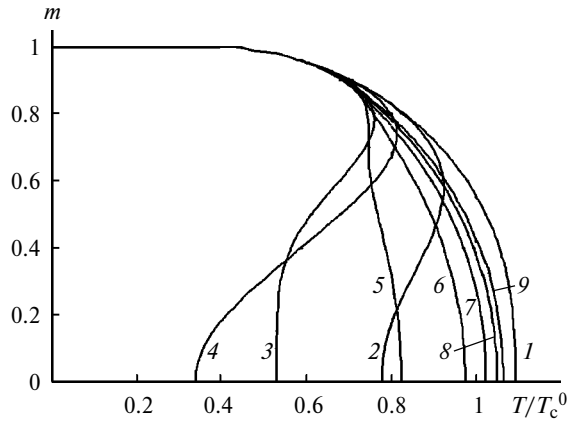


**Fig. 6.** Temperature plot ($T/T_c^0$) of the relative magnetization ($m$) of the oxide nanostructures at different $R/a$: 6 (*1*), 12 (*2*), 25 (*3*), 50 (*4*), 100 (*5*), 200 (*6*), 300 (*7*), 400 (*8*), and 500 (*9*) ($R$ is the cluster radius, $a$ is the lattice increment).

larger than the critical one ($R_{cr}^{max}$), the MPT of the second order characteristic of bulky samples occurs, and $T_C$ increases. A decrease in the cluster size ($<R_{cr}^{min}$) also leads to the MPT of the second order and an increase in $T_C$ due to a decrease in the defect concentration.

The magnetic interaction between clusters affects the MPT character and $T_C$ value. However, a change in the distance between their centers affects the temperature dependence of the magnetization less noticeably than the size change does. Thus, as the distance between clusters was increased from $R$ (see Fig. 6) to the value corresponding to the lattice constant ($a$), the maximum increase in $T_C$ was ~6%. In this case, MPT of the first order become transitions of the second order.

In the framework of the proposed thermodynamic model for MPT related to a change in the defect concentration, the experimental results can be explained as follows. Nanostructurization induced by shear stress under high pressure for systems **1.1** and **1.2** containing α- and γ-$Fe_2O_3$ leads to decreasing the average size of the clusters and distances between their centers. In the case of nanosystem **1.1**, the effect of the cluster size reduction on $T_C$ is compensated by compacting that increases the magnetic field of the clusters. In the case of nanosystems **1.2** or **2.2**, only $T_C$ decreases, and the contribution of the MPT of the first order increases. This is especially pronounced for nanostructure **2.2** in which all ferric oxide nanoclusters lose magnetic ordering at ~20 °C. Thus, an increase in the intercluster distance decreases magnetic interactions, protracts jump-like magnetic transitions, and increases the probability of MPT of the first order.

For sample **2.1** containing metallic Eu, the shear stress under high pressure changes the material nanostructure. Below $T_N$ the starting metal has a domain structure in which the domain size reaches tens of nm.[11] Above $T_N$ ~90 K the MPT of the first order occurs, and metallic Eu loses jumpwise its magnetic ordering. The structure of metallic europium in the magnetically ordered state can be considered as a structure consisting of domains, *viz.*, nanoclusters packed in the metallic Eu lattice. The sizes of these domain-nanoclusters close to 20—30 nm provide the maximum defect density and, hence, the maximum density of strains, which induces the MPT of the first order in metallic Eu. These conclusions are confirmed by high magnetostriction coefficients in rare-earth metals.[22] The shear stress under high pressure decreases the size of the domain-clusters to a value lower than the critical value, decreasing the defect concentration and eliminating strains in the metal. As a result, the MPT of the first order are destroyed and, as a consequence, the magnetically ordered state is extended into a region of higher temperatures. This leads to an increase in $T_N$ for metallic Eu. The addition of 1% ferric oxide clusters to metallic Eu favors an increase in this effect. This effect is due to higher strains of the shear deformation for $Fe_2O_3$ compared to those in metallic Eu, and the strains decrease the sizes of domains composing the nanostructure. This effect is more pronounced after the molecular adamantane clusters are introduced into the Eu matrix. They retain the structure strains after the pressure is removed. In addition, the introduction of an admixture of the $Fe_2O_3$ clusters and adamantane molecules favor, most likely, the uniformity of nanostructurization upon shear stress under high pressure. Thus, nanostructurization of a substance can either decrease or increase $T_C$ ($T_N$) for several substances.

* * *

When the nanostructures based on α- and γ-ferric oxides experience a combination of a lowered critical temperature with an elevated defect concentration created by the shear stress under high pressure, unusual MPT of the first order are observed. The magnetic ordering in the nanosystems disappears jumpwise. In the nanostructures based on metallic europium, the shear stress under high pressure transforms the MPT of the first order characteristic of bulky europium into the MPT of the second order, and the critical temperature increases from ~90 to 100 K. The experimental results agree with the thermodynamic MPT theory predicting a change in the magnetic properties of nanosystems of oxides and metals with a change in the defect concentration. For example, for the nanosystems formed of relatively large clusters 20—50 nm in size, the theory predicts that depending on the defect concentration, cluster size, and intercluster interactions, a change in the character of transition from MPT of the first order to MPT of the second order and a decrease (increase) in the Neel (Curie) points in the nanoclusters can be expected.

This work was financially supported by the Russian Foundation for Basic Research (Project No. 03-03-32029).

## References

1. *Clusters of Atoms and Molecules*, Ed. H. Haberland, Springer-Verlag, Berlin—Heidelberg, 1994, 54.
2. I. P. Suzdalev and P. I. Suzdalev, *Usp. Khim.*, 2001, **70**, 203 [*Russ. Chem. Rev.*, 2001, **70**, 177 (Engl. Transl.)].
3. G. Schmid, *J. Chem. Soc., Dalton Trans.*, 1998, 1077.
4. A. P. Alivisatos, *Science*, 1996, **271**, 933.
5. I. M. Billas, J. A. Becker, A. Chatelain, and W. A. de Heer, *Phys. Rev. Lett.*, 1993, **71**, 4067.
6. A. J. Cox, J. G. Lounerback, S. Eapsel, and L. A. Bloomfield, *Phys. Rev. B*, 1994, **49**, 2295.
7. C. Petit, A. Taleb, and M. P. Pileni, *J. Phys. Chem. B*, 1999, **103**, 1805.
8. L. Thomas, F. Lionti, R. Ballou, D. Gatteshi, R. Sessoli, and B. Barbara, *Nature*, 1996, **383**, 145.

9. C. L. Chien, *Ann. Rev. Mater. Sci.*, 1995, **25**, 129.
10. S. Jin, T. H. Tiefel, M. Mc. Cornack, R. A. Fastnacht, R. Ramesh, and L. H. Chien, *Science*, 1994, **264**, 413.
11. S. V. Vonsovskii, *Magnetizm* [*Magnetism*], Nauka, Moscow, 1971, 1024 (in Russian).
12. S. B. Bean and D. S. Rodbell, *Phys. Rev.*, 1962, **126**, 104.
13. I. P. Suzdalev, *Fiz. Tverd. Tela*, 1970, **12**, 988 [*Sov. Phys. Sol. State*, 1970, **12**, 775 (Engl. Transl.)].
14. Yu. F. Krupyanskii and I. P. Suzdalev, *Zh. Eksp. Teor. Fiz.*, 1974, **67**, 736 [*Sov. J. Exp. Theor. Phys.*, 1974, **38**, 859 (Engl. Transl.)].
15. I. P. Suzdalev, V. N. Buravtsev, V. K. Imshennik, Yu. V. Maksimov, S. V. Novichikhin, A. X. Trauwein, and H. Winkler, *Z. Phys. D*, 1996, **37**, 55.
16. I. P. Suzdalev, Yu. V. Maksimov, V. N. Buravtsev, V. K. Imshennik, A. G. Kazakevich, and S. V. Novichikhin, *Kolloid. Zh.*, 2000, **62**, 257 [*Colloid J.*, 2000, **62**, 224 (Engl. Transl.)].
17. I. P. Suzdalev, Yu. V. Maksimov, S. V. Novichikhin, V. N. Buravtsev, V. K. Imshennik, and V. V. Matveev, *Khim. Fiz.*, 2000, **19**, 105 [*Chem. Phys. Reports*, 2000, **19** (Engl. Transl.)].
18. A. A. Zharov and N. P. Chistotina, *Pribory i tekhnika eksperimenta* [*Instruments and Experimental Technique*], 1974, No. 2, 229 (in Russian).
19. A. G. Kazakevich, A. A. Zharov, P. A. Yampol´skii, and N. S. Enikolopyan, *Dokl. Akad. Nauk SSSR*, 1974, **215**, 1404 [*Dokl. Chem.*, 1974 (Engl. Transl.)].
20. *Chemical Applications of Mössbauer Spectroscopy*, Eds. V. I. Goldanskii and R. H. Herber, Academic Press, New York—London, 1968.
21. P. H. Barret and D. A. Shirly, *Phys. Rev.*, 1963, **131**, 123.
22. K. N. R. Taylor and M. I. Darby, *Physics of Rare Earth Solids*, Chapman and Hall, London, 1972.
23. I. P. Suzdalev, V. N. Buravtsev, V. K. Imshennik, and Yu. V. Maksimov, *Scripta Mater.*, 2001, **44**, 1937.
24. J. K. Vassiliou, V. Mehroya, M. W. Russel, R. D. McMichel, R. D. Shull, and R. F. Ziolo, *J. Appl. Phys.*, 1993, **73**, 5109.
25. I. P. Suzdalev, A. S. Plachinda, V. N. Buravtsev, Yu. V. Maksimov, S. I. Reiman, V. I. Khromov, and D. I. Dmitriev, *Khim. Fiz.*, 1998, **17**, 104 [*Chem. Phys. Reports*, 1998, **17** (Engl. Transl.)].

*Received February 14, 2003;*
*in revised form June 21, 2003*